Applied Physics Letters

RESEARCH ARTICLE | DECEMBER 05 2023

Enhanced current-induced magnetization switching via antiferromagnetic coupled interface in Co/Ho heterostructures FREE

S. M. Li ; H. Y. Poh ; T. L. Jin ; F. N. Tan ; S. Wu ; K. M. Shen ; Y. F. Jiang ; W. S. Lew

Appl. Phys. Lett. 123, 233502 (2023)
https://doi.org/10.1063/5.0174431

AIP Publishing

Applied Physics Letters ARTICLE pubs.aip.org/aip/apl

Enhanced current-induced magnetization switching via antiferromagnetic coupled interface in Co/Ho heterostructures

Cite as: Appl. Phys. Lett. **123**, 233502 (2023); doi: 10.1063/5.0174431
Submitted: 31 August 2023 · Accepted: 18 November 2023 ·
Published Online: 5 December 2023

S. M. Li,[1,2] H. Y. Poh,[1] T. L. Jin,[1] F. N. Tan,[1] S. Wu,[1] K. M. Shen,[1] Y. F. Jiang,[2,a)] and W. S. Lew[1,a)]

AFFILIATIONS

[1]School of Physical and Mathematical Sciences, Nanyang Technological University, 21 Nanyang Link, Singapore 637371, Singapore
[2]Department of Electrical Engineering, School of Internet of Things (IoTs), Institute of Advanced Technology, Jiangnan University, Wuxi 214122, China

[a)]**Authors to whom correspondence should be addressed:** jiangyf@jiangnan.edu.cn and wensiang@ntu.edu.sg

ABSTRACT

Rare-earth ferromagnetic (RE–FM) heterostructures have attracted significant attention due to their intricate spin structures and physical phenomena. The antiferromagnetic coupled (AFC) interface formed by the distinctive interaction between the FM and RE elements has critical contributions to the magnetization reversal process. In this work, we investigate the enhancement of current-induced magnetization switching with the AFC interface at the Co/Ho heterostructure. The results shows that an increased spin–orbit torque (SOT) efficiency of up to 250% was achieved at a Ho thickness of 7 nm, with a critical switching current density of 2.7×10^{10} A/m^2. When a Cu interlayer was introduced between the Co/Ho interface, a decreased SOT efficiency was observed, indicating that the SOT enhancement is primarily attributed to the AFC interfacial effect. At the AFC interface, the interaction between Co and Ho atoms generates an additional torque, enhancing the effective SOT efficiency.

In recent years, the demand for high-efficiency, scalable, and non-volatile spintronic devices has been growing rapidly due to the increasing need for information storage and processing.[1] In this context, the magnetization reversal mechanism induced by spin–orbit torque (SOT) has garnered substantial research interest.[2–5] Previous studies have primarily focused on SOT-induced magnetization reversal in heavy metal (HM)/ferromagnet (FM) heterostructures.[6,7] In these structures, the charge current can be converted into a perpendicular spin current by utilizing the bulk spin Hall effect (SHE) from the HM layer and the Rashba effect induced at the interface.[8,9] This spin current applies a torque to the adjacent FM layer, leading to the reversal of magnetization.[10] The charge-to-spin conversion efficiency in the HM/FM heterostructure is quite low.[11,12] Typically, researchers utilize alloying and inserting antiferromagnetic layers or other materials to enhance spin generation and spin transparency.[13–15] Rare-earth (RE) materials exhibit strong spin–orbit coupling (SOC) effect and a significant exchange coupling effect to the adjacent FM layers, enabling low-power spin manipulation and efficient magnetization switching in SOT devices.[16–18] Studies have shown the presence of Dzyaloshinskii–Moriya interaction (DMI),[19] deterministic current-induced magnetization switching,[20] and strong SOT effects[17] by incorporating RE elements into ferromagnetic metal to form RE–FM alloys or multilayer systems. Magnetic moments of FM and RE, e.g., Gd, Tb, Ho, are antiferromagnetically coupled due to the exchange interactions between 3*d* and 4*f* electrons.[19,21] These coupling effects have a significant impact on the regulation of overall exchange interactions, leading to the generation of exchange fields that have the potential to enhance the SOT effect.[22,23] There have been numerous studies on the tunable bulk exchange interactions based on RE–FM alloys or heterostructures.[17,20,24,25] However, the distinctive interface interactions resulting from the spontaneously formed antiferromagnetic coupled (AFC) interface also exert a measurable influence on the efficiency of spin transmission and magnetization reversal.

In this work, we investigate the influence of the AFC interface at the Ho/Co heterostructure on the enhancement of current-induced magnetization switching. With increasing Ho thickness, the saturation magnetization of the Co/Ho heterostructure decreases, indicating the tunable antiferromagnetic coupling at Co/Ho interface. By introducing a Cu interlayer between the Co and Ho layers, the observed reduction in SOT efficiency confirms the promoting effect of interactions at the Co/Ho interface in driving SOT-induced magnetization reversal.

Thin film stacks of Ti (2 nm)/Pt (4 nm)/Co (1.2 nm)/Ho (t_{Ho} nm)/Ta (4 nm)/Ti (2 nm) were deposited on oxidized Si substrates using high-vacuum magnetron sputtering technique at base pressure of $\sim 3 \times 10^{-8}$ Torr.[26] The bottom Ti layer serves as the adhesion layer between the Pt layer and the substrate. The thickness of the Ho layer (t_{Ho}) was varied from 0 to 7 nm. The top Ta layer has an opposite sign of spin Hall angle with the Pt layer and is used to enhance the SOT efficiency. Figure 1(a) shows schematic of the stack structure. After the film growth, the stacks were patterned into Hall bar devices of $20 \times 200\ \mu m^2$ using the standard photolithography techniques. Figure 1(b) shows the optical image of the patterned device. Ti (10 nm)/Cu (100 nm)/Ti (10 nm) electrode pads were fabricated using liftoff and deposition processes for electric transport measurement purpose.

The magnetic properties of the films were characterized by vibrating sample magnetometer (VSM). Figure 1(c) shows the dependence of the saturation magnetization (M_s) on the Ho layer thickness. The reduction of the measured M_s with the increase in t_{Ho} can be attributed to the spontaneously formed AFC interface at the Co/Ho heterostructures. In the Co/Ho heterostructures, the 4*f* magnetic moments of the RE atoms are coupled with the 3*d* magnetic moments of the FM, which results in the antiparallel alignment of the RE and FM magnetic moments at the interface.[17,27,28] The magnetic moment alignment at the Co/Ho heterostructure is illustrated in the inset of Fig. 1(c). The characteristic of exchange interaction at the interface is the parallel alignment of Co–Co moments and the antiparallel alignment of Co–Ho moments. Furthermore, the enhanced interface atomic mixing at the Co/Ho interface provides possibility for Ho atoms to participate in the interface exchange interaction,[12,18] thereby reducing the overall magnetic moment of the structure. The Ho thickness-dependent coercivity (H_c) and effective anisotropy field (H_k) are plotted in Fig. 1(d). H_k is extracted from the in-plane magnetic field dependence of anomalous Hall resistance (R_{AHE}) according to the Stoner–Wohlfarth model.[26,29] (The fitting detail is shown in Sec. 1 of the supplementary material.) H_c exhibits an increasing trend with larger Ho thickness but subsequently drop after $t_{Ho} = 3$ nm, following the trend of H_k. The trend of H_k as a function of the t_{Ho} suggests that the contribution from the varying t_{Ho} has a coherence length.[19] Further explanation regarding the relationship between H_c and t_{Ho} is presented in Sec. 2 of the supplementary material. In thin film metallic multilayers, the magnetic anisotropy arises from both bulk and interfacial contribution.[30] Hence, by adjusting the t_{Ho}, the interplay between the bulk and interfacial contributions enables the larger H_k at t_{Ho} of 3 nm. The measured anomalous Hall resistance R_{AHE}–H_z loops are shown in Fig. 1(e), where all the Hall bar devices have perpendicular magnetic anisotropy (PMA) property. However, devices with a Ho thickness greater than 7 nm did not exhibit PMA property. The anomalous Hall resistance R_{AHE}–H_z loops with Ho thickness above 7 nm have been shown in Fig. S3 in the supplementary material, Sec. 3.

To investigate the contribution of the Co/Ho interface effect to the SOT efficiency, harmonic Hall measurements were performed on

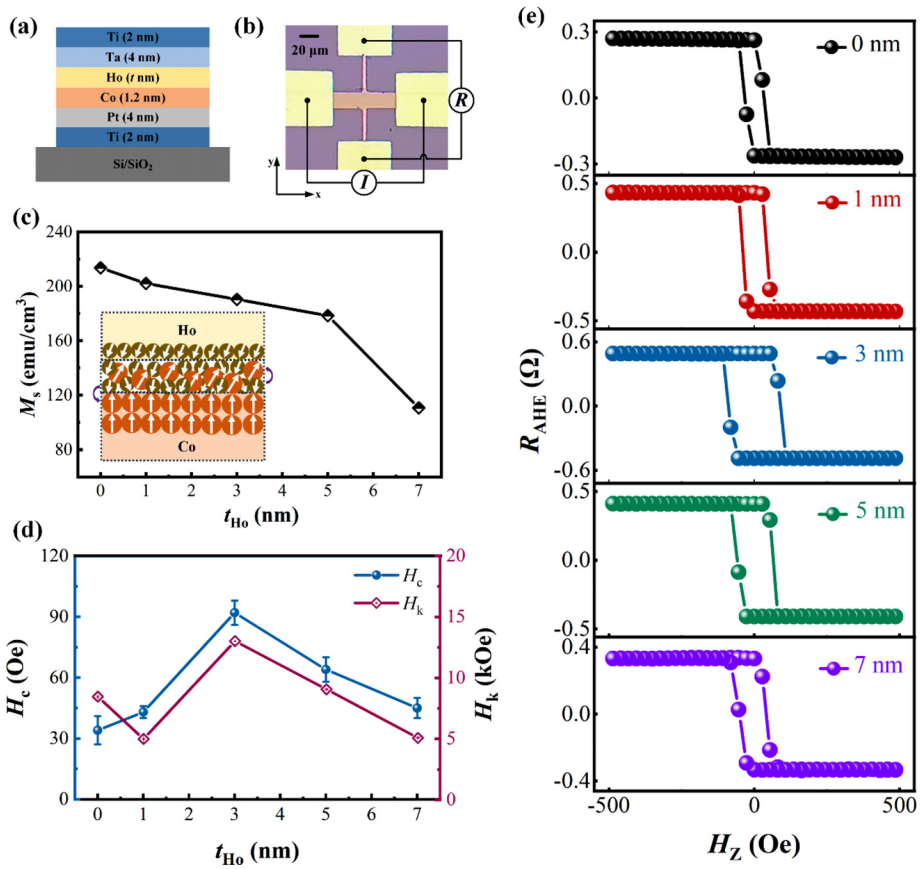

FIG. 1. (a) Schematic of the stack of Ti/Pt/Co/Ho/Ta/Ti multilayer. (b) Optical image of the patterned Hall ball device with schematic of Hall resistance measurement configuration. (c) The M_s obtained from VSM measurements for the deposited films. Inset shows the schematic of magnetic moment alignment at the Co/Ho interface. (d) The H_c and H_k of the devices with different thicknesses of the Ho layer. (e) The measured anomalous Hall resistance R_{AHE}–H_z loops as a function of Ho thickness with current density of $J = 1 \times 10^{10}$ A/m^2.

the Hall bar devices. The measurements were conducted using an alternating current (I_{ac}) source and a lock-in amplifier with a frequency of 307 Hz to detect the Hall voltage (V_H). Figure 2(a) shows schematic of the harmonic Hall voltage measurement setup where an in-plane magnetic field was swept along the current direction (x). The damping-like field (H_{DL}) was extracted from the V_H measurement using the following equation:[31]

$$H_{DL} = -2\left(\frac{dV_{2w}}{dH_x}\right) \Big/ \left(\frac{d^2V_{1w}}{dH_x^2}\right), \quad (1)$$

where V_{1w} and V_{2w} are the first- and second-order harmonic signals, respectively.

Figure 2(b) shows the relationship between the H_{DL} and J of the devices with varying Ho thicknesses. From Fig. 2(b), the H_{DL} per current density ($\chi_{DL} = H_{DL}/J$) is extracted from the slope, and the χ_{DL} as a function of t_{Ho} is summarized in Fig. 2(c). The χ_{DL} exhibits a significant increase with the increasing thickness of the Ho layer. Specifically, when the Ho thickness reaches 7 nm, χ_{DL} increases approximately up to 42 Oe per 10^{10} A/m^2, which is 250% of the samples without the Ho layer. The inset of Fig. 2(c) illustrates the effective spin Hall angle (θ_{SH}) value, where $\theta_{SH} = 2e\mu_0 M_s t_{FM}\chi_{DL}/\hbar$, where e is the electron charge, μ_0 is the permeability vacuum, $\hbar$ is the reduced Planck's constant, and t_{FM} is the thickness of the FM layer. For the Pt/Co/Ta reference sample, the observed value of θ_{SH} (0.128 ± 0.002) is similar to the previously reported values.[32] θ_{SH} increases nearly linearly with the increasing thickness of Ho layer. When the t_{Ho} reaches 7 nm, the θ_{SH} value reaches 0.168 ± 0.001, resulting in an increase to 130% of the samples without the Ho layer. The discrepancy in the enhancement magnitude between the θ_{SH} and χ_{DL} is attributed to the reduction in M_s resulting from the antiparallel alignment of Ho and Co magnetic moments.

Figure 2(d) illustrates the normalized χ_{DL} and $1/M_s$ for various t_{Ho} of the samples, where the current-induced SOT effective field deviates from the $1/M_s$ relation. This disproportionate scaling is attributed to the additional exchange coupling field (H_{EC}) arising from the negative exchange interaction between Co and Ho sublattices at the Co/Ho interface. This H_{EC} adds up with the existing H_{DL}, thereby enhancing the overall effective SOT efficiency.[22] Additionally, the AFC interface between Co and Ho enhances the interface spin-mixing conductance,[33] facilitating the effective interaction of the spins produced in the top layer on the magnetic moments of Co layer. This indicates that the enhancement of SOT efficiency may not solely originate from the bulk effect of Ho layer but also has contribution from the formation of the AFC interface at the Co/Ho heterostructure.

To further investigate the contribution of the AFC interface at the Co/Ho heterostructure to the spin transport, reference samples of Ti (2 nm)/Pt (4 nm)/Co (1.2 nm)/Cu (1.6 nm)/Ho (t_{Ho} nm)/Ta (4 nm)/Ti (2 nm) were fabricated, as schematically shown in Fig. 3(a). Figure 3(b) shows the χ_{DL} of samples with a Cu interlayer at different Ho thicknesses. When the Cu layer is inserted between the Co and Ho layers, the SOT efficiency is significantly reduced to 6–8 Oe per 10^{10} A/m^2 compared to the samples without the Cu interlayer. Although there is a slight increase in χ_{DL} with the increasing t_{Ho}, the magnitude of enhancement remains minimal. Figure 3(c) shows the calculated θ_{SH}, which remains around 0.16 within the range of error. The sample with a Cu interlayer shows a significant increase in M_s compared to the sample without a Cu

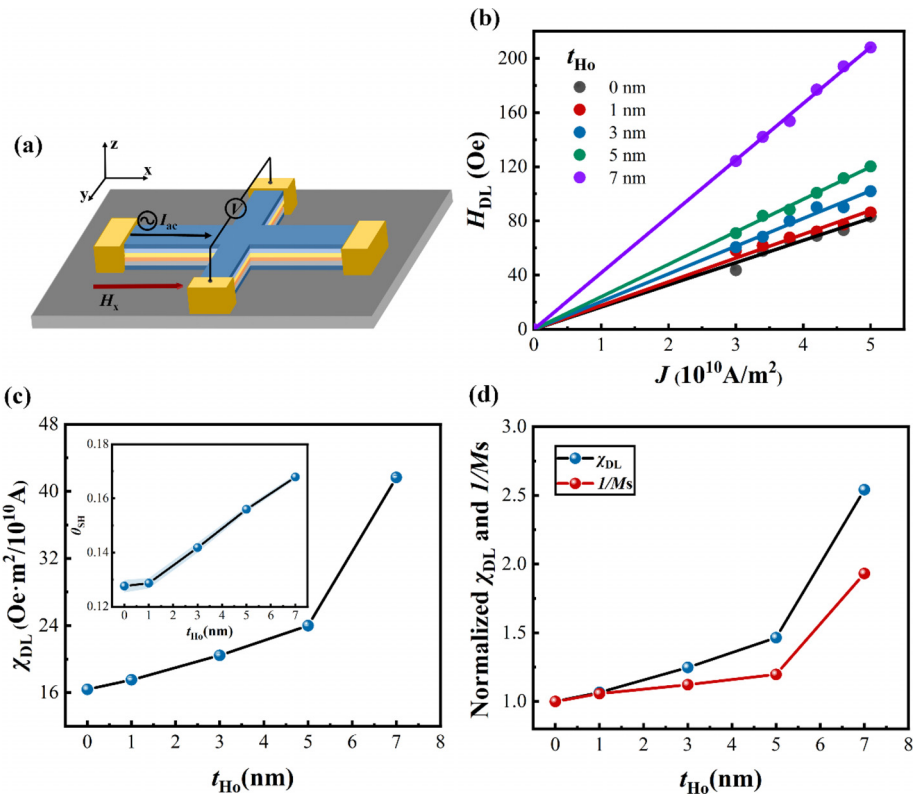

FIG. 2. (a) Schematic of the harmonic measurement setup with a sweeping in-plane field H_x along the current direction x. (b) H_{DL} as a function of the applied current density for devices with various Ho thicknesses. (c) The extracted damping-like effective field per current density χ_{DL} as a function of the Ho thickness. Inset shows the calculated θ_{SH} for the devices with various Ho thicknesses. (d) The normalized values of χ_{DL} and $1/M_s$ with different Ho thicknesses.

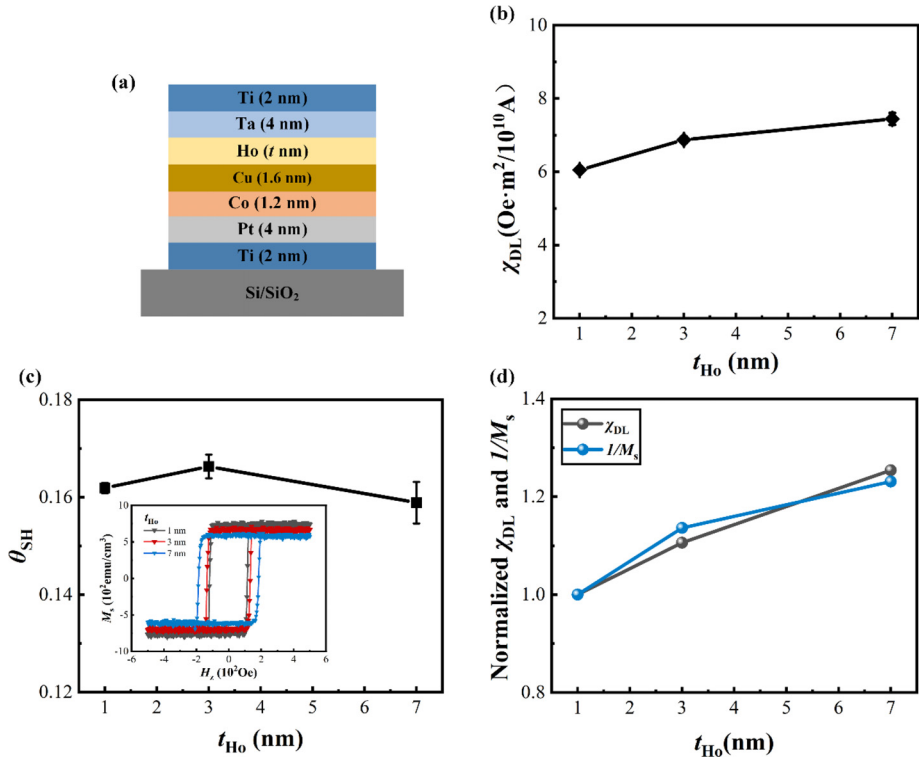

FIG. 3. (a) Schematic of the reference stack with the Cu interlayer. (b) χ_{DL} as a function of Ho thickness for the devices with Cu interlayer. (c) The calculated θ_{SH} as a function of the Ho thickness for the reference samples. The illustration shows the magnetic hysteresis loops in out-of-plane field for devices with various Ho thicknesses. (d) The normalized values of χ_{DL} and $1/M_s$ at different Ho thicknesses for the devices with Cu interlayer.

interlayer. The Cu interlayer at the Co/Ho interface disrupts the antiparallel arrangement of the Co and Ho magnetic moments, resulting in an increase in M_s. Figure 3(d) shows the normalized χ_{DL} and $1/M_s$ for the reference samples. When the Cu interlayer is present, the SOT efficiency follows the trend given by the $1/M_s$ relation. It is known that the spin diffusion length of Cu is above 300 nm, which means the presence of the Cu interlayer effectively disrupts the interaction between Ho and Co atoms at the interface while maintaining spin transport.[34,35] Hence, the

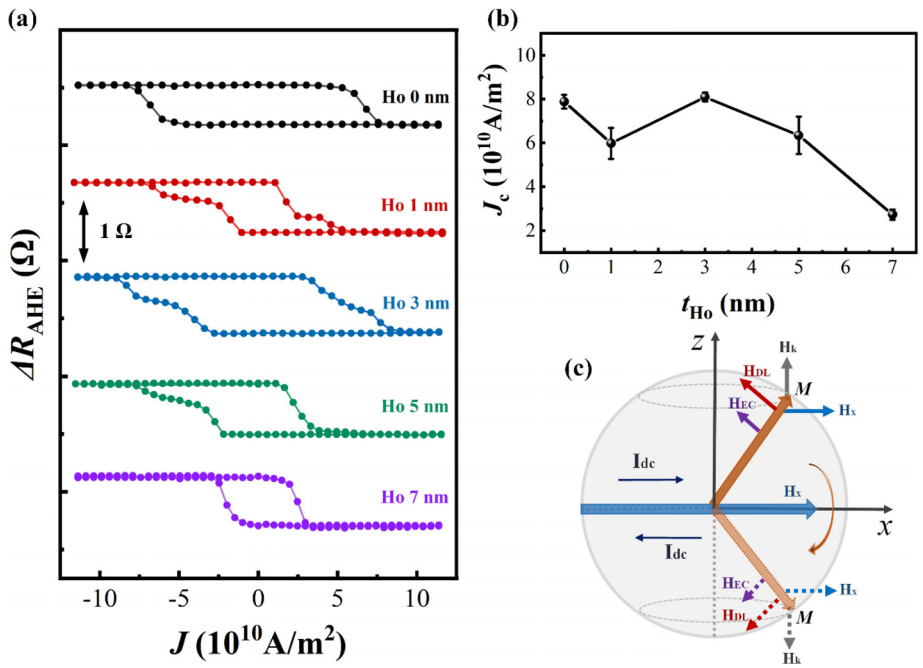

FIG. 4. (a) The measured current-induced magnetization switching loops of the devices with various Ho thickness under $H_x = 1000$ Oe. (b) The extracted J_c as a function of Ho thickness. (c) Schematic of the overall magnetization switching principle in the Co/Ho system.

suppressed SOT efficiency results obtained from the samples with the Cu interlayer indicates that the AFC interface between the Co and Ho is a key factor in enhancing spin transport efficiency.

To gain further insights into the contribution of the AFC interface in the Co/Ho heterostructure to magnetization switching, current-induced switching experiments were conducted. Figure 4(a) shows the R_{AHE}–J loops of the samples with different t_{Ho} with $H_x = 1000$ Oe. J_c is identified as the critical current density for triggering 80% reversal of magnetization state. The observed changes in resistance amplitude are consistent with the observations from the R_{AHE}–H_z loops, indicating deterministic switching of all samples. Figure 4(b) shows the relationship between the extracted J_c and t_{Ho}. In general, J_c decreases with the increase of t_{Ho}. Figure 4(c) shows the diagram of the magnetization switching, the magnetization reversal still predominantly follows the Co sublattice. The magnetization dynamics is determined by the competition among the H_k, the H_{DL}, the H_{EC}, and the H_x. Based on the previous discussion, the interface with antiferromagnetic coupling in the Co/Ho heterostructure contributes to the enhancement of the SOT efficiency. The longitudinal component of the H_{EC} can be combined with the longitudinal component of the H_{DL}, enhancing the effective SOT effect. As the current goes through from the $+x$ to $-x$ direction, accompanied by a reversal in the current direction, the overall magnetization (M) undergoes deterministic reversal. As a result, critical current density of 2.7×10^{10} A/m^2 for the SOT-driven magnetization switching was achieved at $t_{Ho} = 7$ nm, which indicates the potential of Co/Ho heterostructures in low-power applications based on SOT. However, we also observed a decrease in current density when the Ho thickness is equal to 1 nm. This can be attributed to the reduced effective anisotropy, as indicated by the reduced H_k in Fig. 1(d).

In conclusion, the investigation of the SOT effect and the magnetization switching in the Ho/Co heterostructure confirms the critical role of the AFC interface in enhancing current-induced magnetization reversal. Our results demonstrate that the SOT effective field deviates from the $1/M_s$ relation with an increasing Ho thickness, indicating that the interaction between Co and Ho atoms at the Co/Ho interface contributes to the generation of additional torque. Introducing a Cu insertion layer at the Co/Ho interface reduces the SOT efficiency, validating the crucial role of the AFC interface in enhancing SOT efficiency. By studying the current-induced magnetization switching, a critical switching current density of 2.7×10^{10} A/m^2 is demonstrated with a Ho thickness of 7 nm. This work highlights the crucial role of the AFC interface in FM/RE systems for achieving energy-efficient magnetization switching, thereby contributing toward understanding and developing low-power spintronic devices.

See the supplementary material for the extraction of the effective anisotropy field H_k, the hysteresis loops for the thin film samples with different Ho thicknesses, and the measured anomalous Hall resistance R_{AHE}–H_z loops with the Ho thickness of 9 nm.

This work was supported by the NSFC (No. 61774078) and RIE2020 ASTAR AME IAF-ICP Grant (No. I1801E0030).

AUTHOR DECLARATIONS

Conflict of Interest

The authors have no conflicts to disclose.

Author Contributions

Shaomin Li: Conceptualization (equal); Data curation (equal); Formal analysis (equal); Investigation (equal); Methodology (equal); Writing – original draft (equal); Writing – review & editing (equal). **Hanyin Poh:** Conceptualization (equal); Formal analysis (equal); Investigation (equal); Writing – review & editing (supporting). **Tianli Jin:** Conceptualization (equal); Formal analysis (equal); Investigation (equal); Writing – review & editing (supporting). **Funan Tan:** Conceptualization (equal); Formal analysis (equal); Investigation (equal); Writing – review & editing (supporting). **Shuo Wu:** Formal analysis (supporting); Investigation (supporting); Methodology (supporting). **Kaiming Shen:** Formal analysis (supporting); Investigation (supporting); Methodology (supporting). **Yanfeng Jiang:** Funding acquisition (equal); Supervision (equal); Writing – review & editing (equal). **Wen Siang Lew:** Funding acquisition (equal); Supervision (equal); Writing – review & editing (equal).

DATA AVAILABILITY

The data that support the findings of this study are available from the corresponding authors upon reasonable request.

REFERENCES

[1]A. Hirohata, K. Yamada, Y. Nakatani, I.-L. Prejbeanu, B. Diény, P. Pirro, and B. Hillebrands, J. Magn. Magn. Mater. **509**, 166711 (2020).
[2]T. Jin, G. J. Lim, H. Y. Poh, S. Wu, F. Tan, and W. S. Lew, ACS Appl. Mater. Interfaces **14**(7), 9781 (2022).
[3]S. Isogami, Y. Shiokawa, A. Tsumita, E. Komura, Y. Ishitani, K. Hamanaka, T. Taniguchi, S. Mitani, T. Sasaki, and M. Hayashi, Sci. Rep. **11**(1), 16676 (2021).
[4]L. Liu, C. Zhou, T. Zhao, B. Yao, J. Zhou, X. Shu, S. Chen, S. Shi, S. Xi, D. Lan, W. Lin, Q. Xie, L. Ren, Z. Luo, C. Sun, P. Yang, E. J. Guo, Z. Dong, A. Manchon, and J. Chen, Nat. Commun. **13**(1), 3539 (2022).
[5]C. Song, R. Zhang, L. Liao, Y. Zhou, X. Zhou, R. Chen, Y. You, X. Chen, and F. Pan, Prog. Mater. Sci. **118**, 100761 (2021).
[6]Y. Takeuchi, C. Zhang, A. Okada, H. Sato, S. Fukami, and H. Ohno, Appl. Phys. Lett. **112**(19), 192408 (2018).
[7]J. Yu, X. Qiu, W. Legrand, and H. Yang, Appl. Phys. Lett. **109**(4), 042403 (2016).
[8]J. Sinova, S. O. Valenzuela, J. Wunderlich, C. H. Back, and T. Jungwirth, Rev. Mod. Phys. **87**(4), 1213 (2015).
[9]L. Liu, O. J. Lee, T. J. Gudmundsen, D. C. Ralph, and R. A. Buhrman, Phys. Rev. Lett. **109**(9), 096602 (2012).
[10]I. M. Miron, K. Garello, G. Gaudin, P. J. Zermatten, M. V. Costache, S. Auffret, S. Bandiera, B. Rodmacq, A. Schuhl, and P. Gambardella, Nature **476**(7359), 189 (2011).
[11]H. Y. Poh, C. C. I. Ang, G. J. Lim, T. L. Jin, S. H. Lee, E. K. Koh, F. Poh, and W. S. Lew, Phys. Rev. Appl. **19**(3), 034012 (2023).
[12]S. Woo, M. Mann, A. J. Tan, L. Caretta, and G. S. D. Beach, Appl. Phys. Lett. **105**(21), 212404 (2014).
[13]D. M. Polishchuk, Y. O. Tykhonenko-Polishchuk, Y. M. Lytvynenko, A. M. Rostas, O. V. Gomonay, and V. Korenivski, Phys. Rev. Lett. **126**(22), 227203 (2021).
[14]L. Zhu, D. C. Ralph, and R. A. Buhrman, Phys. Rev. B **99**(18), 180404 (2019).
[15]H. Wang, J. Finley, P. Zhang, J. Han, J. T. Hou, and L. Liu, Phys. Rev. Appl. **11**(4), 044070 (2019).
[16]R. Bansal, N. Chowdhury, and P. K. Muduli, Appl. Phys. Lett. **112**(26), 262403 (2018).
[17]Q. Y. Wong, C. Murapaka, W. C. Law, W. L. Gan, G. J. Lim, and W. S. Lew, Phys. Rev. Appl. **11**(2), 024057 (2019).
[18]Q. Chen, L. Cao, J. Li, Q. Fu, Y. Zhu, Q. Guo, R. Liu, T. Li, W. Zhang, J. Du, J. Zheng, Z. Huang, P. K. J. Wong, B. Fang, Z. Zeng, and Y. Zhai, Appl. Phys. Lett. **120**(24), 242405 (2022).

[19]L. Liu, X. Zhao, W. Liu, Y. Song, X. Zhao, and Z. Zhang, Nanoscale **12**(23), 12444 (2020).
[20]Y. Wu, X. Zeng, Y. Guo, Q. Jia, B. Wang, and J. Cao, Appl. Phys. Lett. **118**(2), 022401 (2021).
[21]K. Ueda, M. Mann, P. W. P. de Brouwer, D. Bono, and G. S. D. Beach, Phys. Rev. B **96**(6), 064410 (2017).
[22]R. Mishra, J. Yu, X. Qiu, M. Motapothula, T. Venkatesan, and H. Yang, Phys. Rev. Lett. **118**(16), 167201 (2017).
[23]Y. Xu, S. Tong, J. Lu, D. Wei, and J. Zhao, Appl. Phys. Lett. **118**(25), 252405 (2021).
[24]B. Hebler, A. Hassdenteufel, P. Reinhardt, H. Karl, and M. Albrecht, Front. Mater. **3**, 8 (2016).
[25]P.-W. Lee, C.-C. Huang, S. Mangin, and C.-H. Lai, J. Magn. Magn. Mater. **563**, 169879 (2022).
[26]F. N. Tan, Q. Y. Wong, W. L. Gan, S. H. Li, H. X. Liu, F. Poh, and W. S. Lew, J. Magn. Magn. Mater. **485**, 174 (2019).
[27]Y. Liu, Z. Xu, L. Liu, K. Zhang, Y. Meng, Y. Sun, P. Gao, H. W. Zhao, Q. Niu, and J. Li, Nat. Commun. **13**(1), 1264 (2022).
[28]W. Zhang, D. Zhang, P. K. Wong, H. Yuan, S. Jiang, G. van der Laan, Y. Zhai, and Z. Lu, ACS Appl. Mater. Interfaces **7**(31), 17070 (2015).
[29]S. Emori, E. Martinez, K.-J. Lee, H.-W. Lee, U. Bauer, S.-M. Ahn, P. Agrawal, D. C. Bono, and G. S. D. Beach, Phys. Rev. B **90**(18), 184427 (2014).
[30]M. T. Johnson, P. J. H. Bloemen, F. J. A. den Broeder, and J. J. de Vries, Rep. Prog. Phys. **59**(11), 1409 (1996).
[31]M. Hayashi, J. Kim, M. Yamanouchi, and H. Ohno, Phys. Rev. B **89**(14), 144425 (2014).
[32]J. Yun, D. Li, B. Cui, X. Guo, K. Wu, X. Zhang, Y. Wang, Y. Zuo, and L. Xi, J. Phys. D **51**(15), 155001 (2018).
[33]J. Liang, Q. Chen, Q. Guo, W. Jiang, Z. Huang, B. You, J. Du, and Y. Zhai, Appl. Phys. Lett. **121**(19), 192402 (2022).
[34]S. Yakata, Y. Ando, T. Miyazaki, and S. Mizukami, Jpn. J. Appl. Phys., Part 1 **45**(5A), 3892 (2006).
[35]C. Du, H. Wang, F. Yang, and P. C. Hammel, Phys. Rev. Appl. **1**(4), 044004 (2014).